Shear dispersion

W. R. Young and Scott Jones

Citation: Physics of Fluids A **3**, 1087 (1991); doi: 10.1063/1.858090
View online: http://dx.doi.org/10.1063/1.858090
View Table of Contents: http://scitation.aip.org/content/aip/journal/pofa/3/5?ver=pdfcov
Published by the AIP Publishing

Shear dispersion

W. R. Young
Scripps Institution of Oceanography, La Jolla, California 92093
Scott Jones
Sibley School of Mechanical and Aerospace Engineering, Cornell University, Ithaca, New York 14853-7501

(Received 10 September 1990; accepted 7 November 1990)

This review of shear dispersion emphasizes that the usual one-dimensional diffusion equation, derived by Taylor [Proc. R. Soc. London Ser. A **219**, 186 (1953)], is an asymptotic result that is valid only at large time. One route to earlier validity is a systematic wave-number expansion based on the center manifold theorem. This procedure captures much of the early behavior but it does discard exponentially decaying transients. However, in some cases of practical importance, such as tracer release experiments in rivers, the observation of "anomalous diffusion" (i.e., tracer variance growing nonlinearly with time) is at odds with this asymptotic reduction. Alternative approximations and models, which account for exponential transients using a description that is nonlocal in time are reviewed. A secondary theme of this review is the application of shear dispersion to mixing of passive and active scalars in rivers and estuaries. An example is shear dispersion of salt in which the shear flow is created by salinity gradients. Other examples include fixed flux convection.

I. INTRODUCTION

In 1953, Taylor published a remarkable paper on the dispersion of a passive scalar ("tracer") by laminar Poiseuille flow in pipe.[1] The problem is to develop a quantitative theory for the spread of tracer along the axis of the pipe, while avoiding the detailed solution of the advection–diffusion equation

$$c_t + uc_x = D\nabla^2 c. \tag{1}$$

In Eq. (1), $c(x,y,z,t)$ is the concentration of scalar, $u(y,z) = 2(U/a^2)(a^2 - y^2 - z^2)$ is the axial velocity along the pipe, and D is the molecular diffusivity of the tracer.

Taylor's theory of "shear dispersion" focuses on the sectionally averaged concentration $C(x,t)$ and shows that, at large times, this quantity satisfies a simpler advection–diffusion equation:

$$C_t + UC_x = D_{\text{eff}} C_{xx}, \tag{2}$$

where

$$C(x,t) \equiv \frac{1}{A}\int c(x,y,z,t)\,dA \quad \text{and} \quad U \equiv \frac{1}{A}\int u(y,z)\,dA. \tag{3}$$

Here, D_{eff} is an "effective diffusivity" and Taylor finds

$$D_{\text{eff}} = D + U^2 a^2/48D. \tag{4}$$

[Taylor's heuristic derivation of Eqs. (2)–(4) assumes that the Péclet number $P \equiv aU/D$ is large so that the first term on the right-hand side of Eq. (4) is much smaller than the second. The complete expression in Eq. (4) was given by Aris.[2] There are mistaken claims in the literature that Eq. (4) applies only when the Péclet number is small, so that the second term on the right-hand side is a small enhancement of D.]

In going from Eq. (1) to Eq. (2), the number of independent variables has been reduced from four to two, and the the concept of an effective diffusivity for the averaged concentration is very appealing. Equation (2) has been extensively used by hydrologists, physiologists, chemical engineers, and many other practical-minded scientists. At a fundamental level, Taylor's result is a good example of a general mathematical technique: the simplification of a complicated system by the elimination of "fast modes." Taylor's problem is discussed from this perspective in Sec. II.

It must be stressed that Eq. (2) is an asymptotic result. In an initial value problem, in which the tracer is released in some arbitrary configuration, the reduced description in Eq. (2) is valid only when $t \gg a^2/D$. At large times, molecular diffusivity mixes the tracer in the transverse direction while the shear stretches it out in the axial direction. Thus if the concentration is written as

$$c(x,y,z,t) = C(x,t) + c'(x,y,z,t), \tag{5}$$

then, at large times, the transverse differences in concentration represented by c' are much less than the axial variations contained in C. This observation is at the heart of Taylor's derivation of Eq. (2) and is essential in more complicated problems with dynamically active scalars such as buoyancy (see Sec. III).

A heuristic derivation of Eq. (2) begins by sectionally averaging Eq. (1) to obtain

$$C_t + UC_x + \overline{u'c'_x} = DC_{xx}, \tag{6}$$

where the overbar is a sectional average (e.g., $\bar{u} = U$) and u' is defined by analogy with c' in Eq. (5). Subtracting Eq. (6) from Eq. (1) gives a rather complicated equation for c', but when $t \gg a^2/D$ there is a simple dominant balance:

$$u'C_x \approx D(c'_{yy} + c'_{zz}). \tag{7}$$

Equation (7) has a compelling physical interpretation: Transverse variations in concentration are created by the shear flow tilting and stretching the averaged concentration and these same variations are destroyed by transverse molec-

 0899-8213/91/051087-15$02.00

ular diffusion. Because C does not depend on the transverse coordinates, it is easy to solve Eq. (7) for c'. The correlation $\overline{u'c'}$ in Eq. (6) is then seen to be proportional to C_x and evaluating the integral one obtains Eqs. (2) and (4). Notice that both c' and $\overline{u'c'}$ vary inversely with D, which explains the inverse proportionality in the last term of Eq. (4).

Scale analysis of the complete c' equation shows that the dominant balance in Eq. (7) depends on *two* different approximations. First, one requires $a/l \ll 1$, where l is the axial length over which variations in c occur. In particular, there is no restriction on the size of $P = aU/D$, provided that the aspect ratio a/l is sufficiently small. For instance, with *a posteriori* scale analysis, one can show that the ratio of a neglected term, such as $u'c'_x$, to a retained term, for instance, $u'C_x$, is aP/l. This becomes small as $t \to \infty$ and the tracer is spread over a large axial distance.

The second approximation used in Eq. (7) is that the time scale of evolution of C and u' be much longer than the transverse diffusion time a^2/D. If this condition is not satisfied, then the term c'_t must be retained in Eq. (7). An example is given in Sec. IV B. Other examples include the shear dispersion by time periodic velocity fields.[3,4] If $u(z,t)$ has a period that is comparable to the transverse diffusion time, then c'_t is not negligible, even though the average field C is evolving on a much longer time scale.

Batchelor[5] remarks that the referees who first received Taylor's paper on shear dispersion could not fail to recognize "the fundamental character of the result that differential unidirectional convection and transverse diffusion together yield a longitudinal diffusion process far downstream." In fact, this article is the most frequently cited of Taylor's works—see Fig. 1. We emphasize the importance of the restriction to *unidirectional* velocity fields. Of the two approximations discussed above, the first is essential and depends crucially on the anisotropy of the velocity. The second approximation can be avoided at the expense of solving a time dependent diffusion equation in the transverse plane.

Figure 1 also shows citations of two other papers[6,7] on dispersion by Taylor. In 1954, Taylor applied a similar analysis to tracer dispersion in turbulent Poiseuille flow.[6] Once again, the evolution of the sectionally averaged concentration is described by Eq. (2) but the reasoning used to obtain D_{eff} is less compelling than that in the earlier discussion of laminar Poiseuille flow. In the turbulent case, Taylor gives an estimate based on the Reynold's analogy

$$D_{\text{eff}} \approx 10.1 a u_*, \tag{8}$$

where u_* is the friction velocity.

While Taylor's experiments in the laminar and turbulent cases generally supported his theory, there were some discrepancies. In both the laminar and turbulent experiments the measured concentration profiles show "persistent skewness," i.e., concentration measured at a fixed point as a function of time has a long tail, as in Fig. 2. This difficulty is more pronounced in the turbulent case and Taylor attributed it to tracer retention in the viscous sublayer so that transverse mixing is incomplete. The implication is that, in Taylor's experiments, Eq. (2) is inaccurate because insufficient time has elapsed—a conclusion drawn by Chatwin[8] and reinforced with a model that accounts for tracer retention in the viscous sublayer.

The conclusion that the diffusion approximation in Eq. (2) becomes valid only after a time of order a^2/D is correct. However, an incorrect corollary, that the transient is associated with incomplete transverse mixing, is sometimes drawn. In fact, there are cases in which the transverse variations in concentration are very small and yet Eq. (2) is not valid. Some explicit examples are given in Sec. IV. In general, thorough transverse mixing is necessary, but not sufficient, for the validity of the Taylor diffusion equation. The correct physical condition for the validity of Taylor's approximation is that every element of tracer has had time to sample the entire cross section of the flow.

Many authors since Chatwin have attempted to improve Taylor's theory to obtain earlier validity, and experiments, particularly in rivers, have shown that some improve-

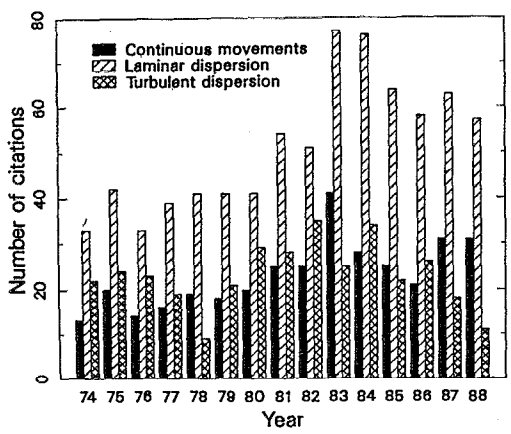

FIG. 1. Citations of three papers (Ref. 1, 6, and 7) by Taylor.

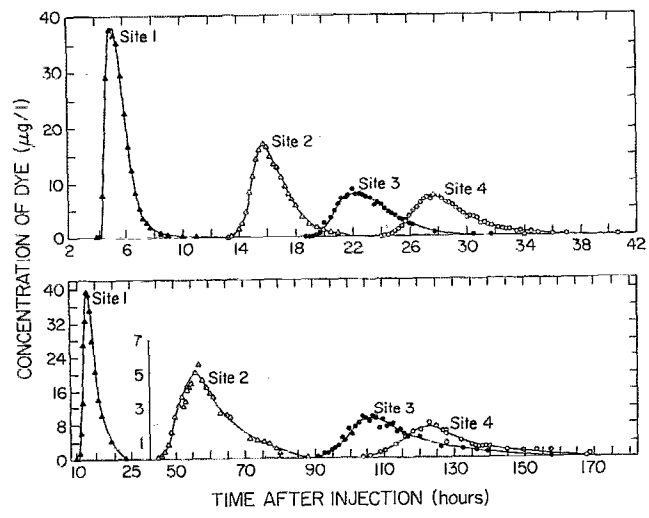

FIG. 2. This figure, reproduced from Ref. 39, shows field measurements in the Monacy River (top panel) and the Amite River (lower panel). In both cases, concentration is recorded as a function of time at fixed sites downstream from a release point. The long tail on the concentration records (persistent skewness) indicates that the Taylor limit has not been achieved.

ment is necessary. Indeed, many experimental investigators would probably argue that the predictions of Eq. (2) are so at variance with experience that alternative theories are required. The review by Chatwin and Allen[9] is a good summary of research on the dispersion of pollutants in natural waterways.

In Sec. II, we review some recent work that builds on Eq. (2) as the first term in a systematic expansion. In Sec. III, we discuss some problems in which a dynamically active tracer, such as buoyancy, is dispersed by a shear flow driven by its own gradients. In Sec. IV, we review the tracer release experiments in rivers in more detail and present some theoretical models of *nondiffusive* dispersion by a unidirectional velocity field.

II. A WAVE-NUMBER EXPANSION FOR SHEAR DISPERSION

In this section, we review some recent developments that provide a systematic route to the approximation in Eq. (2). These developments, mainly due to Roberts and collaborators in Refs. 10–13 improve on the approximation in Eq. (2) by adding terms of higher order in a wave-number expansion, e.g., $D_3 C_{xxx}$, etc. Indeed, even Eq. (2), as it currently stands, is not complete because the initial condition is not known. Even though $C = \bar{c}$, the appropriate initial condition for Eq. (2) is *not* $\bar{c}(x,y,z,0)$. This surprising point is explained with specific examples in the next subsection.

A. Initial displacement and variance deficit

Aris[2] realized that it is easy to obtain a closed hierarchy for the axial moments

$$c_p(y,z,t) \equiv \int_{-\infty}^{\infty} x^p c(x,y,z,t)\,dx \tag{9}$$

of the concentration directly from Eq. (1). To find each c_p, one must solve a diffusion equation in the transverse plane. Using Fourier–Bessel series, Aris calculated up to $p = 3$ and provided exact results that can be used to assess the accuracy of the approximation in Eq. (2).

The center of mass of the tracer is

$$x_m \equiv \frac{\int xc\,dV}{\int c\,dV} = \frac{\int c_1\,dA}{\int c_0\,dA}. \tag{10}$$

Aris found that if the initial release is a point delta function $c(x,y,z,0) = \delta(x)\delta(y - y_0)\delta(z - z_0)$, at a distance $r_0 = \sqrt{y_0^2 + z_0^2}$ from the axis of the pipe, then

$$x_m = Ut + (Pa/24)(2 - 6r_0^2 + 3r_0^4) + \text{E.S.T.} \tag{11}$$

The first term on the right-hand side is the transport of the tracer downstream by the sectionally averaged velocity. The second term is the *initial displacement* of the center of mass. The last term (E.S.T.) is exponentially small as $t \to \infty$. The initial displacement depends on the position of the point release and reflects the transport of the tracer in the early phase of shear dispersion. If we solve Eq. (2) with the initial condition $C(x,0) = \bar{c}(x,y,z,0) = \delta(x)$, we get the inaccurate result $x_m = Ut$. There is an order one error (the initial displacement) which does not disappear as $t \to \infty$.

Of course a point release is the harshest test of a theory that assumes that the tracer is well mixed across the section of the pipe. But it is also possible to solve the the moment hierarchy with an initial condition $c(x,y,z,0) = \delta(x)$. Indeed in this case, in which the tracer is initially uniform in the transverse section, the initial displacement is zero. That is, one finds the exact result $x_m = Ut + \text{E.S.T.}$ so that the errors in the prediction of x_m from Eq. (2) with $C(x,0) = \delta(x)$ are exponentially small as $t \to \infty$.

However, there is a problem with sectionally uniform releases that appears when one calculates the variance

$$\sigma^2 \equiv \frac{\int (x - x_m)^2 c\,dV}{\int c\,dV} = \frac{\int c_2\,dA}{\int c_0\,dA} - x_m^2 \tag{12}$$

from the moment hierarchy. With $c(x,y,z,0) = \delta(x)$, the exact result is

$$\sigma^2 = 2D_{\text{eff}}\,t - a^2P^2/360 + \text{E.S.T.} \tag{13}$$

The second term on the right-hand side is the *variance deficit* and, like the initial displacement, it reflects early dispersion.

Now if Eq. (2) is solved with the initial condition $C(x,0) = \bar{c}(x,y,z,0) = \delta(x)$, then the inaccurate result $\sigma^2 = 2D_{\text{eff}}\,t$ follows. Thus changing the initial condition so that the release is sectionally uniform has merely deferred the difficulty from the center of mass to the variance.

Based on evidence such as this, Frankel and Brenner[14] concluded that a systematic improvement of Eq. (2) is not possible. However, following Mercer and Roberts,[12] we argue that there is a cure for Eq. (2) that ensures that its predictions for the moments agree with the exact results apart from terms that decay exponentially as $t \to \infty$. That is, the method of Mercer and Roberts[12] gives exact expressions for the initial displacement and variance deficit. And when higher-order gradient terms such as $D_3 C_{xxx}$ are incorporated, the method provides this same exponential accuracy for the skewness. The key is that a consistent expansion results not only in additional terms such as $D_3 C_{xxx}$ in Eq. (2), but also in a wave-number expansion of the initial condition so that $C(x,0) = \bar{c}(x,y,z,0) + E_1 \partial_x c(x,y,z,0) + \cdots$.

B. Advantages of the center manifold approach

The method of Mercer and Roberts[12] is based on the center manifold theorem. Obtaining the initial displacement and variance deficit is a relatively minor success for this powerful method. In fact, these results have been obtained in the past using a variety of different approaches:

(i) Aris[2] using the moment method summarized above.

(ii) Chatwin,[15] who developed an asymptotic solution of Eq. (1) by an expansion in powers of $t^{-1/2}$.

(iii) Frankel and Brenner[14] using "generalized Taylor dispersion theory." In the classic Taylor problem discussed above, this specializes to an ingenious calculation of the moments that avoids the Fourier–Bessel series used by Aris.

(iv) Smith[16] using a "delay–diffusion" equation that, in execution, requires the same eigenfunction expansions as (i) and (ii). We return to Smith's approach in Sec. IV.

The expansion based on the center manifold theorem is algebraically simpler than all of the above, but this hardly justifies the detailed derivation given below. Instead, we empha-

size the following advantages of the center manifold machinery:

(i) The theory can easily be extended to encompass gradual axial variations in pipe diameter, diffusivity, and so on. Unlike (ii) and (iii) above, there is no restriction on the transverse structure of the initial conditions and there are no extra complications in treating a time dependent source.

(ii) Nonlinear problems (such as the shear dispersion of buoyancy[17] or chemically reacting tracers[18]) are contained in the same framework.

(iii) The calculation of higher-order corrections is structurally simple and can be done by computer. Mercer and Roberts[12] calculate up to D_{24} using the algebra manipulation package REDUCE. Standard techniques can then be used to estimate the radius of convergence of the wave-number expansion.

C. The expansion

In this review, we do not attempt a systematic exposition of the center manifold theorem[19] (CMT) but instead we apply in a cookbook fashion to the particular problem of shear dispersion. Our approach is motivated by Mercer and Roberts[12] but does not follow them closely in execution. Some readers may prefer the more formal development in Ref. 10–12, though we believe the following development is useful pedagogically both as nontrivial application of the center manifold theorem and as a conclusive resolution of what Frankel and Brenner[14] called "a long-standing puzzle in longitudinal dispersion theory."

The essential idea is that the modes of Eq. (1), obtained by substituting $c = \exp(-st + ikx)\hat{c}(y,z)$, decay at different rates. The most slowly decaying mode is the branch that has $s = 0$ and $\hat{c} = 1$ when $k = 0$. (Note that the no flux boundary conditions at the pipe wall are essential for this neutral mode.) When k is slightly different from zero, this mode decays on the slow time scale k^2/D. In addition to the slow mode, there are more rapidly decaying branches with nontrivial transverse structure at $k = 0$. These fast modes decay on the time scale a^2/D, i.e., the transverse diffusion time across the channel. The CMT assures us that it is possible to "filter" the rapidly decaying modes and obtain a simplified dynamics, such as Eq. (2), which describes the long time evolution of the slow mode with exponential accuracy.

Of course Eq. (1) is linear, so that the modes as described above are uncoupled and decay independently. The second ingredient is to use the modal structure at $k = 0$, i.e., $\hat{c}(y,z) = 1$, even though k is slightly different from zero (i.e., long but not infinite horizontal scales). When this is done, the modes (or "quasimodes") are coupled and this coupling produces the effective diffusivity.

This procedure described above is executed by assuming the ansatz

$$c(x,y,z,t) = C(x,t) + [\alpha_1(y,z)\partial_x + \alpha_2(y,z)\partial_x^2 + \cdots]C(x,t) + R(x,y,z,t). \tag{14}$$

The first term on the right-hand side has the trivial transverse structure of the $k = 0$ neutral mode. The remaining terms are

$$c' = \mathcal{L}C + R, \quad \text{where } \mathcal{L} \equiv \alpha_1(y,z)\partial_x + \alpha_2(y,z)\partial_x^2 + \cdots \tag{15}$$

is an operator that commutes with ∂_x and ∂_t. The functions $\alpha_n(y,z)$ will be determined systematically as the procedure unfolds. Here, c' contains all of the rapidly decaying modes with transverse structure.

Equation (15) appears at the moment as an unmotivated assumption about the asymptotic structure of the solution. From the perspective of the CMT, it is obtained by, first, Fourier transforming Eq. (1) with respect to the spatial variable x. Thus $\partial_x \to ik$, and one then appends a trivial evolution equation: $\dot{k} = 0$. This trick enables one to regard the terms $ikc(k,y,z,t)$ and $-Dk^2c(k,y,z,t)$ in the transformed version of Eq. (1) as nonlinear. Linearizing this expanded nonlinear system for $\dot{k}$ and $\dot{c}$ shows that there are actually two neutral modes, viz., $(c,k) = (1,0)$ and $(c,k) = (0,1)$. The amplitudes of these two modes are the master variables to which the decaying modes are slaved. The ansatz in Eq. (15) is the untransformed form of this relation and is a Taylor series expansion in the small amplitude of the $(c,k) = (0,1)$ mode. For more details see Mercer and Roberts.[12]

Thus the philosophy behind the approach in Eqs. (14) and (15) is that, as $t \to \infty$, there is a "master" variable $C(x,t)$ [this is the amplitude of the $(c,k) = (1,0)$ mode] whose evolution is determined from Eq. (2), and the remainder of the solution, the "slave" variable c', is related diagnostically to the master through $c' = \mathcal{L}C$. However, because of forcing or initial conditions in general, one must include the term R, which is a "remainder" or "displacement" of the slave variables away from the exact center manifold relation $c' = \mathcal{L}C$. For instance, in an initial value problem, $c'(x,y,z,0)$ and $C(x,0)$ will usually be specified so that the system is displaced away from the center manifold. Here, R represents this displacement or remainder. In a pure initial value problem, in which there is no source of tracer other than the pulse that sets up the initial condition, R decays exponentially as the system settles onto the center manifold. On the other hand, if there is a sustained source, injecting tracer at different instants, then the solution is constantly being tugged away from the center manifold and R does not decay. Cox and Roberts[13] provide a general discussion of the CMT for forced dynamical systems, while the development below is specialized to shear dispersion.

Apart from the final term R, the ansatz in Eq. (14) is similar to the "separation of variables" expansion introduced heuristically by Gill and Sankarasubramanian.[20] [In this reference, the functions α_n depend on t as well as y and z (see also Smith[16]). This is an attempt to obtain earlier validity of the expansion. In the present development, this is accomplished by a systematic treatment of R.] Frankel and Brenner[14] showed that, without the inclusion of R, the ansatz is incapable of systematically improving the leading order approximation in Eq. (2). This emphasizes the importance of correctly incorporating R into the expansion.

We consider a slight extension of Eq. (1) by allowing for an arbitrary external source of tracer:

$$c_t + uc_x = D\nabla^2 c + s. \tag{16}$$

Initial conditions are contained as a special case, $s(x,y,z,t) = c(x,y,z,0)\delta(t)$. Other extensions, such as a nonconstant diffusivity or a tracer that sediments, are easily included in the formalism.

Sectionally averaging Eq. (16), we have for the master variable

$$C_t + UC_x + \overline{u'c'_x} - DC_{xx} = S, \tag{17}$$

where $S(x,t)$ is the sectional average of $s(x,y,z,t)$, defined in analogy with U and C in Eq. (3). For the slave variable,

$$c'_t + Uc'_x + (u'c' - \overline{u'c'})_x - D\nabla^2 c' = -u'C_x + s'. \tag{18}$$

Substituting Eq. (15) into Eq. (17), we find for the master variable

$$C_t + UC_x - (D_{\text{eff}} C_{xx} + D_3 C_{xxx} + \cdots) = S - \overline{u'R_x}, \tag{19}$$

where

$$D_{i+1} \equiv -\overline{\alpha_i u'} \quad \text{and} \quad D_{\text{eff}} = D + D_2. \tag{20}$$

Now substitute Eqs. (15) and (19) into Eq. (18) and separate the terms proportional to R from those proportional to C so that

$$D\nabla_T^2 \mathcal{L} C = u'C_x + (u'\mathcal{L} C_x - \overline{u'\mathcal{L} C_x}) - \mathcal{L}\,\overline{u'\mathcal{L} C_x}, \tag{21}$$

and for the remainder

$$R_t + UR_x + (u'R - \overline{u'R})_x - \mathcal{L}\,\overline{u'R_x} - D\nabla^2 R = s' - \mathcal{L} S. \tag{22}$$

In Eq. (21), $\nabla_T^2 \equiv \partial_y^2 + \partial_z^2$ is the transverse part of the Laplacian. Equations (19), (21), and (22) are exact consequences of (16). Simplification is possible because of the separation in time scales noted above. We also have a small parameter: The wave number k of the master mode is very close to zero, or equivalently, ∂_x is small.

Equation (21) determines the functions $\alpha_j(y,z)$. Collecting equal powers of ∂_x^n, one has for the first two terms

$$D\nabla_T^2 \alpha_1 = u' \quad \text{and} \quad D\nabla_T^2 \alpha_2 = -\overline{u'\alpha_1} + u'\alpha_1, \tag{23}$$

and thereafter

$$D\nabla_T^2 \alpha_n = -\overline{u'\alpha_{n-1}} + u'\alpha_{n-1} + \sum_{j=1}^{n-2} \alpha_j D_{n-j}. \tag{24}$$

The boundary conditions in Eqs. (23) and (24) are $\nabla_T \alpha_j \cdot \mathbf{n} = 0$ (i.e., no-flux) and we also note that $\overline{\alpha}_j = 0$. Because of the self-adjoint form of the left-hand side of Eqs. (23), one can obtain D_3 without explicitly solving for α_2:

$$D_3 \equiv -\overline{u'\alpha_2} = -\overline{u'\alpha_1^2}. \tag{25}$$

A similar trick works at higher orders—given α_n, one can obtain D_{n+2} as a bonus.

The evolution equation for the remainder, Eq. (22), can be solved in the same way. One writes

$$R = R_0 + \epsilon R_1 + \cdots, \quad \text{where } \partial_x \text{ and } \partial_t \sim \epsilon. \tag{26}$$

Collecting powers of ∂_x we have for the first two orders

$$D\nabla_T^2 R_0 = -s'$$

and

$$D\nabla_T^2 R_1 = (\partial_t + U\partial_x) R_0 + \partial_x (u'R_0 - \overline{u'R_0}) + \alpha_1 \partial_x S. \tag{27}$$

In the final evolution equation, Eq. (19), we require only $\overline{u'R}$ and again we can take advantage of the self-adjoint form to avoid explicit solution of Eq. (27). For instance, it is easy to show that

$$\overline{u'R_0} = -\overline{\alpha_1 s'} \quad \text{and} \quad \overline{u'R_0\alpha_1} = -\overline{\alpha_2 s'}, \tag{28}$$

and introducing $D\nabla_T^2 \beta_1 \equiv \alpha_1$, one finds that

$$\overline{u'R_1} = -(\partial_t + U\partial_x)\,\overline{\beta_1 s'} + \overline{\alpha_1^2}\,\partial_x S - \partial_x\,\overline{\alpha_2 s'}. \tag{29}$$

Thus, to second-order, the evolution equation is

$$C_t + UC_x = D_{\text{eff}} C_{xx} + S + \partial_x\,\overline{\alpha_1 s'} + \partial_x^2 (\overline{\alpha_2 s'} - \overline{\alpha_1^2} S) + (\partial_t + U\partial_x)\partial_x\,\overline{\beta_1 s'}. \tag{30}$$

Apart from exponentially decaying transients, this equation gives the exact evolution of the second moment and second cumulant from an arbitrary initial condition. In the next subsection, we compare its predictions with some well-known exact results for the classic Taylor problem.

D. Poiseuille flow in a circular tube

For the classical Taylor problem, which is dispersion by Poiseuille flow in a circular pipe, one obtains from Eq. (23)

$$\begin{aligned} \alpha_1 &= -(Pa/24)(2 - 6\hat{r}^2 + 3\hat{r}^4), \\ \alpha_2 &= (P^2a^2/11\,520) \\ &\quad \times (31 - 180\hat{r}^2 + 300\hat{r}^4 - 200\hat{r}^6 + 45\hat{r}^8), \end{aligned} \tag{31}$$

where $\hat{r} \equiv r/a$ and $P \equiv Ua/D$ is the Péclet number.

In Sec. II A, we noted that a point release at a distance r_0 from the axis leads to the initial displacement of the center of mass given by the third term in Eq. (11). From Eq. (31), we recognize that Eq. (11) is $x_m = Ut - \alpha_1(r_0)$ + E.S.T. and with $s = \delta(x)\delta(y - y_0)\delta(z - z_0)\delta(t)$ this same result is obtained from Eq. (30).

If $s' = 0$, then the calculation of R is simpler (e.g., $R_0 = 0$, $R_1 = \beta_1 \partial_x S$, etc.) and for the classic Taylor problem it is easy to improve Eq. (30) by one extra term in the wave-number expansion. One finds

$$\begin{aligned} (\partial_t + U\partial_x) C - \left(D + \frac{P^2 D}{48}\right) C_{xx} + \frac{P^3 Da}{2880} C_{xxx} \\ = S - \frac{P^2 a^2}{720} S_{xx} + \frac{17P^3 a^3}{322\,560} S_{xxx} \\ + \frac{13P^2 a^4}{138\,240D} (\partial_t + U\partial_x) S_{xx}. \end{aligned} \tag{32}$$

In the earlier discussion surrounding Eq. (13), the initial release was given by $s = S = \delta(t)\delta(x)$. Adopting this forcing function in Eq. (32), one finds that the center of mass is $x_m = Ut$ and this agrees with the earlier calculation

using the moment method. For the variance, Eq. (32) gives

$$\sigma^2 = \frac{\int_{-\infty}^{\infty} (x - Ut)^2 C(x,t)\,dx}{\int_{-\infty}^{\infty} C(x,t)\,dx} = 2D_{\text{eff}}\,t - \frac{P^2 a^2}{360}, \tag{33}$$

which also agrees with the exact result in Eq. (13), apart from the exponentially small terms. Finally, for the third cumulant, we recover Chatwin's[15] result

$$\int_{-\infty}^{\infty} (x - Ut)^3 C\,dx = \frac{P^3 Da}{480}\,t - \frac{17 P^2 a^3}{53\,760}. \tag{34}$$

Chatwin[15] found not only the simple expressions for the variance and third moment given in Eqs. (33) and (34), but he also calculated the exponentially small corrections. Using a comparison with this exact solution, he concluded that the exponentially small terms are negligible when $Dt/a^2 > 0.2$. To get information about the higher moments and cumulants, such as the kurtosis, one must calculate more terms in the wave-number expansion such as $D_4 C_{xxxx}$.

Finally, the expansion above can be extended to capture the exponentially small terms by including additional master variables. A possibility is to use the amplitudes of two or more of the most slowly decaying modes as master variables. The result is coupled advection–diffusion equations for these amplitudes. One approach to this calculation is given by Smith.[21] An alternative is discussed below in Sec. IV, where the exponential transients are captured by a single equation that is, however, nonlocal in time.[16,22]

Section III is an intermezzo in which we review density-driven shear dispersion. The formulation is informal and heuristic although a more systematic approach along the same lines as the present section is possible.

III. SHEAR DISPERSION OF DENSITY

In this section, we discuss the shear dispersion of a dynamically active tracer: density or buoyancy. We represent the density ρ of the fluid as

$$\rho = \rho_0 (1 - g^{-1} b), \tag{35}$$

where g is the acceleration of gravity and b is the "buoyancy." The shear flow that disperses buoyancy is driven by the buoyancy gradients themselves and the result is a nonlinear diffusion equation. This process was first discussed by Erdogan and Chatwin[17] in 1967. Since then, it has been rediscovered in a variety of different configurations and often not recognized as an example of shear dispersion. The goal of this section is to heuristically derive the "Erdogan–Chatwin" equation and discuss some of its applications to estuarine dynamics and convection in cavities.

A. Shear dispersion of buoyancy in a shallow horizontal layer of fluid

We begin with an elementary pedagogical problem: a shallow layer of fluid with nonuniform density is in a two dimensional container (depth d and length l) with insulated walls. The fluid is diffusive and viscous so that, ultimately, all density variations within the container disappear. When $l \gg d$, this process takes place on two disparate time scales.

The fast process is vertical diffusion over the depth d of the layer and, as in the Introduction, this results in a buoyancy profile in which

$$b(x,z,t) = B(x,t) + b'(x,z,t) \quad \text{with } b' \ll B, \tag{36}$$

where $B(x,t)$ is the vertically averaged buoyancy defined in analogy with Eq. (3). The vertical momentum balance is hydrostatic so that

$$p(x,z,t) \approx p_B(x,t) + \rho_0 B(x,t) z, \tag{37}$$

where the constant of integration p_B is the bottom ($z = 0$) pressure.

The slow process is lateral shear dispersion of buoyancy. Following arguments originated by Erdogan and Chatwin[17] we show below that the slow process of lateral mixing is described by a nonlinear diffusion equation

$$B_t = \kappa B_{xx} + \alpha (B_x^3)_x, \tag{38}$$

where κ is the molecular diffusivity of the buoyant contaminant. The constant α is

$$\alpha = \frac{1}{362\,880} \frac{d^8}{\nu^2 \kappa}. \tag{39}$$

The dependence of α on the eighth power of the layer depth is notable. Some properties of Eq. (38) in the strongly nonlinear limit ($\kappa = 0$) are discussed by Smith[23] and this reference also reviews earlier work on the mathematical properties of Eq. (38).

For the moment, we suppose that there are end walls on the cavity so that the volume flux past any section is zero

$$U = \frac{1}{d} \int_0^d u\,dz = 0. \tag{40}$$

If the density varies over a length $l \gg d$, then the lateral pressure gradients $\partial_x p = \partial_x p_B + \rho_0 z\,\partial_x B$ are balanced by vertical stresses, i.e., $p_x/\rho_0 \approx \nu u_{zz}$. The scaling arguments justifying this balance are the same as those in lubrication theory. Thus, with no slip conditions at $z = 0$ and d, we find the horizontal velocity

$$\nu u' = (B_x/12)(2z^3 - 3dz^2 + d^2 z), \tag{41}$$

where Eq. (40) was used to determine $\partial_x p_B$. The vertically averaged buoyancy equation is

$$B_t + \overline{u'b'} = \kappa B_{xx} \tag{42}$$

and to calculate the second term we first obtain b' from the analog of Eq. (7). The result is

$$b' = (B_x^2/1440\nu\kappa)(12z^5 - 30dz^4 + 20d^2 z^3 - d^5) \tag{43}$$

and evaluating $\overline{u'b'}$ we obtain Eqs. (38) and (39).

It is easy to relax the restriction in Eq. (40) and allow for a net flow, driven, for instance, by a pressure gradient. The resulting evolution equation is

$$B_t + UB_x = \kappa_{\text{eff}} B_{xx} + \alpha (B_x^3)_x, \tag{44}$$

where κ_{eff} given by a relation analogous to Eq. (4). [In Eq. (44), it is assumed that the boundary conditions at the top and bottom of the layer are both no-slip. If there is a stress-free upper boundary and a no-slip lower boundary, then the velocity profile is no longer symmetric about the middle of

the layer and, as a result, there is a quadratic nonlinear term $(B_x^2)_x$ on the right-hand side of Eq. (44).]

Our derivation has been informal, although using the methods of Sec. II, a more rigorous development is possible. The most important point to note is that the inequality in Eq. (36) demands that the fastest time scale in Eq. (38) be much longer than the transverse mixing time d^2/κ. In the interesting nonlinear case, we can estimate the time scale from Eq. (38) as $l^4/(\Delta B)^2\alpha$, where ΔB is the scale of horizontal buoyancy variations in the layer. Then, from Eq. (39), if this is to be much greater than d^2/κ, one must have

$$\nu^2\kappa^2 l^4/d^{10}(\Delta B)^2 \gg 1. \tag{45}$$

In the preceding discussion, we considered an initial value problem in which the buoyancy ultimately becomes uniform. However, the approximations used above are also central to a number of convection problems in which motion is sustained by heating and cooling the boundary of a cavity. For instance, Cormack *et al.*, in Refs. 24–26, studied the convection driven in a shallow layer of fluid by heating one side wall and cooling the other, while the top and bottom are insulated. In the central portion of the cavity, far away from the diabatic side walls, the solution is given by Eqs. (39) and (41) with a uniform buoyancy gradient B_x. Indeed, because $B_{xx} = 0$, the velocity is unidirectional and this is an exact solution of the full equations of motion. Thus the steady version of Eq. (38) describes the transfer of heat from one end wall to the other, and we see that, in the strongly nonlinear limit, the flux is proportional to the *cube* of the gradient.

Another class of problems in which shear dispersion of buoyancy is important is fixed flux convection.[27–29] If the heat flux is prescribed at the top and bottom of the layer, then the most unstable mode has infinite horizontal wavelength. (This is in contrast to the classic Rayleigh–Bénard problem in which the temperature is prescribed and the most unstable mode has a horizontal wavelength comparable to the layer thickness d.) Once again, the extreme aspect ratio of the flow hints that shear dispersion is likely to be important and indeed the finite amplitude evolution equations in Refs. 27–29 all contain the nonlinear diffusion term $(B_x^3)_x$, which is symptomatic of buoyancy-driven shear dispersion.

B. Dynamics of well-mixed estuaries

Models such as Eq. (44) have been used to describe the distribution of salinity in a well-mixed estuary (for example see Smith[30] and Godfrey[31]). The classic field study of such a system is Pritchard's[32–34] analysis of the James River Estuary. Two of his illustrations are reproduced in Figs. 3 and 4. Figure 3 contrasts the surface salinity in the estuary at two phases in the tidal cycle. It is this strong tidal flow that generates the small-scale turbulence that is actually responsible for mixing the buoyancy vertically and, in the calculation above, this is modeled by the eddy mixing coefficients κ and ν. Figure 4 shows that the vertical buoyancy variations are much weaker than the variations along the axis of the estuary [as asserted in Eq. (36)] so that the contours of surface salinity in Fig. 3 are actually good approximations to the vertically averaged salinity. Because of the horizontal variations in salinity, the fractional change in density is of order

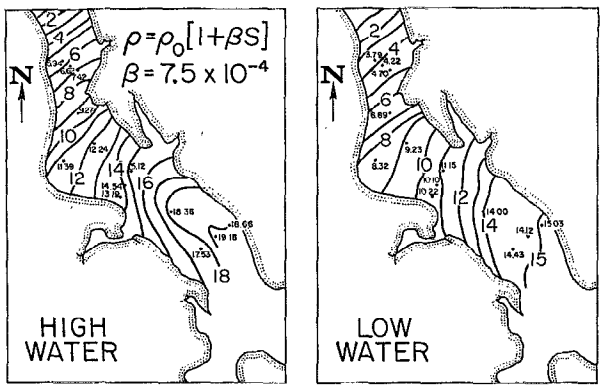

FIG. 3. This figure, reproduced from Ref. 32, shows surface salinity in the James River Estuary. The variation in salinity along the axis estuary produces fractional changes in density of the order of 1%. The units are salinity in parts per thousand by mass.

1.5%. It is the pressure gradient associated with this horizontal nonuniformity in buoyancy that drives a recirculating estuarine flow [as in Eq. (41)] in which fresh surface water moves seaward and deep salty water landward. As a result this recirculating flow transfers salt away from the ocean.

Of course the net flux of salt up the James River must be zero. This balance is possible because salinity flux associated with the vertically averaged flow U cancels the salinity flux of the recirculating flow described in the previous paragraph. Specifically, from Eq. (44), we have in the steady state

$$UB - \kappa_{\text{eff}} B_x - \alpha B_x^3 = 0. \tag{46}$$

When the last term on the left-hand side is negligible, one has the well-known no-flux solution of the linear diffusion equation. For instance, if the mouth of the river is $x = 0$ and the ocean occupies $x > 0$, and has fixed buoyancy $B_0 < 0$, then in the river

$$B = B_0 e^{Ux/\kappa_{\text{eff}}} \quad \text{if } x < 0. \tag{47}$$

However, Pritchard's observations show that the relevant case for the James River is the complementary limit in which the first and third terms in Eq. (44) balance. (In the

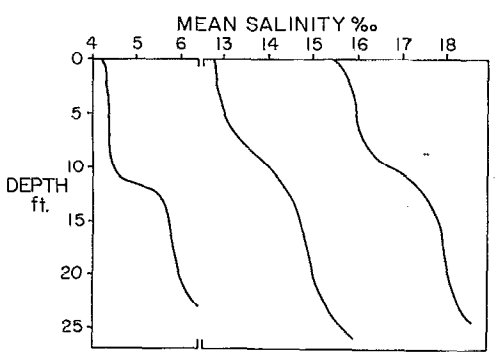

FIG. 4. Vertical sections of salinity in the James River Estuary show that the salinity is much more thoroughly mixed in the vertical than in the horizontal. The units are the same as in Fig. 3. The important point is that the vertical variation in salinity is roughly 2 parts per thousand while, in the axial direction, the salinity variations are of order 18 parts per thousand.

James River, u' is of order 5 cm sec^{-1}, while U is two orders of magnitude smaller.) Then, following Godfrey,[3] the solution is

$$B = B_0[1 + (x/\xi)]^{3/2} \quad \text{if} \quad -\xi < x < 0,$$
$$B = 0 \quad \text{if} \quad x < -\xi, \tag{48}$$

where $\xi \equiv (\frac{3}{2})|B_0|^{2/3}(\alpha/U)^{1/3}$. This is a grossly simplified model of the salinity distribution at the mouth of a well-mixed estuary. Complications, such as variations in depth, tidal turbulence parametrizations, and Coriolis force, have all been ignored in favor of presenting a simplified model that emphasizes the importance of buoyancy-driven shear dispersion. Perhaps the most important process that has been ignored is the transverse circulation driven by horizontal density variations across the channel (i.e., in the y direction). Figure 3 shows these are of order 2 parts per thousand, which is the same order as the vertical variations in Fig. 4. Thus there is circulation driven by both the longitudinal and transverse density variations. Smith[30] has formulated a model of this three-dimensional flow, which is relevant to estuaries.

IV. PREASYMPTOTIC DISPERSION

Analysis of tracer release experiments in rivers has relied heavily on Eq. (2) and simple extensions of it. Invariably, the comparison between theory and experiment has been unsatisfactory. The usual explanation is that the theory does not apply because insufficient time has elapsed. The observations summarized below in Sec. IV A seem to disagree so strongly with Eq. (2), and even with the improvements discussed in Sec. II, that alternative models are suggested. In this section, we review both the experiments and some of the theoretical models that describe "preasymptotic dispersion." We use this term to denote a regime in which the exponentially decaying transients (the terms E.S.T. in Sec. II) are not small.

Besides dispersion in rivers, there are many other contexts in which preasymptotic effects are important. Engineers deal with flow and mixing in very complicated geometries such as packed beds. Physiologists are interested in transport through capillary networks. In these systems, a macroscopic description, analogous to Eq. (2), is obtained by averaging over the microscale geometry. But once again this diffusive description only applies at very long times. We restrict attention to dispersion in unidirectional velocity fields and do not attempt a detailed review of these allied fields. We refer the reader to an excellent collection of recent reviews in the volume edited by Guyon *et al.*[35] and to the articles by Koch and Brady.[22,36–38]

A. Tracer release experiments in natural streams

Nordin and Sabol[39] compiled the results of 51 tracer release experiments in North American rivers. In some of these experiments, the variance defined in Eq. (12) grew nondiffusively

$$\sigma^2 \sim t^{2\beta} \tag{49}$$

with $\beta \approx 0.7$. Power laws, such as Eq. (49), are often referred to as *anomalous diffusion*. The case $\beta > \frac{1}{2}$ is *superdiffusive* and $\beta < \frac{1}{2}$ is *subdiffusive*. The observation of anomalous diffusion disqualifies Eq. (2) [or the extensions of it, such as Eq. (32)] as an adequate model. One-dimensional transport equations with constant coefficients predict that variance grows linearly as in Eq. (13).

Other experiments in the suite analyzed by Nordin and Sabol[39] did exhibit a linear increase of variance with time, i.e., $\beta = \frac{1}{2}$. One might be tempted to conclude that, at least in some experiments, there is support for the diffusion model in Eq. (2). This view is frustrated by a later contribution in which Nordin and Troutman[40] show that, in some experiments in which the variance grows diffusively, the temporal skewness coefficient does not agree with the predictions of Eq. (2). We discuss Nordin and Troutman[40] in more detail below.

Similar results, both anomalous diffusion and persistent skewness, were reported by Day[41] in an analysis of five tracer release experiments in small mountain streams in New Zealand. He states unequivocally that Eq. (2) is not an adequate model. Valentine and Wood[42] argued that in a natural stream there is often a stationary eddy structure next to the bed that traps tracer and so protracts the preasymptotic regime. They suggested that many rivers are simply not long enough for Taylor's theory to work. Day and Wood,[43] in a further analysis of the data from New Zealand, reached the intriguing conclusion that the concentration profile is self-similar, but not Gaussian, as the tracer moves downstream.

Both anomalous diffusion and persistent skewness have often been attributed to tracer retention in quasistagnant regions. In a river there are lagoons, recirculating eddies, junked cars, beaver dams, and fallen trees and all are responsible for trapping tracer and protracting the approach to the Taylor limit. "Dead-zone" models attempt to account for the cumulative effects of these obstacles by partitioning the total concentration of tracer $C(x,t)$ into two parts:

$$C = f + g, \tag{50}$$

where f is free, actively transporting tracer and g is trapped. Thus tracer conservation is

$$f_t + g_t + Uf_x = Df_{xx}, \tag{51}$$

so that only gradients in f are responsible for transport. The second relation between f and g is usually taken to be capacitance coupling

$$g_t = \mu(\epsilon f - g), \tag{52}$$

or, if all of the tracer is released in the untrapped region at $t = 0$, then

$$g(x,t) = \epsilon\mu \int_0^t f(x,\tau) e^{\mu(\tau - t)}\, d\tau. \tag{53}$$

Sundaresan *et al.*[44] remark that this is an "old and honorable problem whose solution has been rediscovered many times under various guises." A complete review would lead us into chemical engineering, soil science, physiology, etc. In the chemical engineering literature,[36,22] the term "hold-up dispersion" refers to an analogous class of phenomena in which tracer is trapped in recirculating pockets or in permeable particles, etc. In the context of river dispersion, Nordin and

Troutman[40] and Valentine and Wood[42] are relevant references. In the following discussion, we provide a slightly more general development by replacing Eq. (53) with

$$g(x,t) = \int_0^t K(t-\tau) f(x,\tau) d\tau. \tag{54}$$

For a discussion of the physical basis of this class of models, see Young.[45] Here, we just remark that the kernel $K(t)$ is essentially the distribution of waiting times in the dead zones. The exponential kernel in Eq. (53) corresponds to the very special case of tracer arrest with a constant probability per time of escape. In other examples, such as those in Ref. 45, the kernel has a much slower power law decay as $t \to \infty$.

Nordin and Troutman[40] concluded that the dead-zone model was incapable of explaining the field observations. Their argument is powerful and will be recapitulated and generalized here. The field observations, such as those in Fig. 2, are measurements of concentration as a function of time at several fixed points (usually four to six) downstream from the tracer release. From these observations, Nordin and Troutman calculated the first three temporal moments of the data:

$$\langle t^n \rangle \equiv \frac{\int_0^\infty C(x,t) t^n \, dt}{\int_0^\infty C(x,t) \, dt}, \quad \text{for } n = 1,2, \text{ and } 3, \tag{55}$$

at the observation points. These same temporal moments can be computed analytically from the model in Eqs. (52) and (53). One then attempts to determine the model parameters U, D, μ, and ϵ by matching these two results. The difficulty is that the model predicts that the normalized temporal skewness,

$$S_k(x) \equiv s_k / \sigma_{\text{time}}^{3/2},$$

where

$$\sigma_{\text{time}}^2 \equiv \langle (t - \langle t \rangle)^2 \rangle \quad \text{and} \quad s_k \equiv \langle (t - \langle t \rangle)^3 \rangle, \tag{56}$$

decays like $x^{-1/2}$, where x is the distance downstream from the release. The data show that $S_k(x)$ is constant, i.e., independent of x.

This observation is a strong criticism of the model in Eqs. (52) and (53) and one response is that, perhaps, the generalization in Eq. (54) can explain the persistent skewness. In fact, this more elaborate model is easily solved with Laplace transforms and one finds as $x \to \infty$

$$\begin{aligned} \langle t \rangle &\sim (1 + k_0)(x/U), \\ \sigma_{\text{time}}^2 &\sim 2[k_1 + \alpha(1 + k_0)^2](x/U), \\ s_k &\sim 3[4\alpha^2(1 + k_0)^3 + 4\alpha(1 + k_0)k_1 + k_2](x/U), \end{aligned} \tag{57}$$

where

$$\alpha \equiv D/U^2 \quad \text{and} \quad k_n \equiv \int_0^\infty t^n K(t) dt. \tag{58}$$

Thus, provided the kernel decays quickly enough to ensure that $k_2 < \infty$, this whole class of models is disqualified by the observation of persistent skewness.

Another failure of the dead-zone model is that it does not predict superdiffusive spreading of the tracer. Young[45] showed that an algebraically decaying kernel in Eq. (54) results in subdiffusive dispersion. The observations indicate that the superdiffusive case [e.g., $\beta = 0.7$ in Eq. (49)] is the relevant one.

The dead-zone model above has been introduced in an *ad hoc* fashion without any attempt to relate it directly to detailed fluid mechanics. For more careful derivations, see Purnama[46,47] and Smith.[48] But the essential point is that the dead-zone model is not able to account for either the persistent temporal skewness or the superdiffusive dispersion evident in some field observations.

With this motivation we turn to a review of some theoretical models of superdiffusive dispersion in unidirectional velocity fields. We emphasize the importance of the restriction to unidirectional fields. The models below are distinguished from other examples of anomalous diffusion in fluid mechanics (such as those of Koch and Brady[37,38]) by the fact that the tracer samples the velocity field through molecular diffusion, rather than through random advection by a spatially disordered velocity field.

Finally, the phenomenon of anomalous diffusion is not restricted to fluid mechanics and the literature is enormous. Good reviews from the perspective of statistical physics and chemistry are Montroll and Shlesinger,[49] Montroll and West,[50] and Haus and Kehr.[51]

B. Preasymptotic shear dispersion in random velocity fields

In this subsection, we discuss a class of models that show how shear dispersion in a random velocity field leads to superdiffusive dispersion and persistently non-Gaussian concentration densities. Following de Marsily and Matheron,[52] who were concerned with modeling tracer dispersion in aquifers, we consider solutions of Eq. (1) and suppose that $u(z)$ is a realization from an ensemble of random velocity fields. Specifically, the domain is periodic in z with wavelength Λ and

$$u(z) = \sum_{j=-\infty}^{\infty} u_k e^{ikz},$$

where

$$k \equiv (2\pi/\Lambda) j \quad \text{and} \quad j = \cdots -1, 0, 1, \cdots. \tag{59}$$

Here, u_k is a random variable satisfying the reality condition $u_k = u^*_{-k}$, where $*$ denotes the complex conjugate. For simplicity, we assume that $u_0 = 0$ so that there is no net translation in any realization. Using $\langle\ \rangle$ to denote the ensemble average, the mean-square velocity is

$$u_{\text{rms}}^2 = \sum_k \langle u_k u_k^* \rangle \approx \int_{-\infty}^{\infty} S(k) dk, \tag{60}$$

where $dk \equiv 2\pi/\Lambda$ and the velocity spectrum is

$$S(k) \equiv (\Lambda/2\pi) \langle u_k u_k^* \rangle. \tag{61}$$

We now follow the heuristic argument from the Introduction and obtain an evolution equation for the zero wavenumber component of the concentration field. In any particular realization, we represent the solution of Eq. (1) as

$$c(x,z,t) = \sum_k c_k(x,t) e^{ikz} = c_0(x,t) + c'(x,z,t). \tag{62}$$

We suppose that the initial condition in every realization is $c(x,z,0) = \delta(x)$ so that the tracer is thoroughly mixed in the transverse direction. The analog of Eq. (6) is

$$\partial_t c_0 + \partial_x \overline{uc'} = D\,\partial_x^2 c_0, \tag{63}$$

where now the overbar denotes integration over a period: $\overline{f} \equiv \Lambda^{-1}\int f\,dz$. To obtain c' in terms of c_0, we solve the analog of Eq. (7):

$$\partial_t c' - D\,\partial_z^2 c' = -u\,\partial_x c_0, \tag{64}$$

with the initial condition $c'(x,z,0) = 0$. To capture the exponentially decaying transients, we have retained the time derivative $\partial_t c'$ in Eq. (64). Thus we do *not* require that the evolution of the concentration is slow relative to the transverse diffusion time Λ^2/D. However, we do consistently neglect the terms $\partial_x(uc' - \overline{uc'})$ because these are of order as $\partial_x^2 c_0$, rather than $\partial_x c_0$. The solution of Eq. (67) is straightforward and one finds

$$\overline{uc'} = -\sum_k u_k u_k^* \int_0^t e^{-Dk^2(t-t')}\partial_x c_0(x,t')\,dt'. \tag{65}$$

The final step is to ensemble average Eq. (65). This gives

$$\langle \overline{uc'} \rangle = -\int_0^t K(t-t')\partial_x C(x,t')\,dt', \tag{66}$$

where $C(x,t) \equiv \langle c_0(x,t) \rangle$ and

$$K(\tau) = \sum_k \langle u_k u_k^* \rangle e^{-Dk^2\tau} \approx \int_{-\infty}^{\infty} S(k) e^{-Dk^2\tau}\,dk. \tag{67}$$

To obtain Eq. (66), we have consistently neglected a correlation $\langle u_k u_k^* \tilde{c}_0 \rangle$, where $\tilde{c}_0 \equiv c_0 - C$. Once again this neglected term is higher order in ∂_x.

The final evolution equation,

$$\partial_t C = D\,\partial_x^2 C + \int_0^t K(t-t')\partial_x^2 C(x,t')\,dt', \tag{68}$$

is nonlocal in time.[16,22,45,53] On very long times, of order Λ^2/D, it simplifies to a diffusion equation with

$$D_{\text{eff}} = D + \int_0^\infty K(\tau)\,d\tau = D + D^{-1}\int_{-\infty}^{\infty} k^{-2} S(k)\,dk. \tag{69}$$

However, before this limit is reached there may be a prolonged period of anomalous diffusion. To illustrate this, we consider a model spectrum which is nonzero only when $0 < k_1 < |k| < k_2$. In this band of wave numbers, we suppose that

$$S(k) = S_0 k^{-\alpha}, \tag{70}$$

where

$$u_{\text{rms}}^2 = [2S_0/(1-\alpha)](k_2^{1-\alpha} - k_1^{1-\alpha}),$$

and $-1 \leqslant \alpha \leqslant 1$.

On intermediate times, $(k_2^2 D)^{-1} \ll t \ll (k_1^2 D)^{-1}$, the kernel in Eq. (67) is

$$K(\tau) \approx \Delta/\Gamma(\nu)\tau^{1-\nu}, \tag{71}$$

where we have introduced

$$\nu \equiv (\alpha+1)/2$$

and

$$\Delta \equiv \pi(1-\nu)D^{\nu-1}u_{\text{rms}}^2/\sin(\pi\nu)(k_2^{2-2\nu} - k_1^{2-2\nu}). \tag{72}$$

Because $-1 \leqslant \alpha \leqslant 1$, the exponent ν in Eq. (71) is in the interval $0 \leqslant \nu \leqslant 1$.

It is now easy to calculate the evolution of the spatial moments from Eqs. (68) and (71). Assuming the normalization $\int C\,dx = 1$, one finds for the second moment

$$\int x^2 C\,dx = 2Dt + [2\Delta/\Gamma(\nu+2)]t^{\nu+1}. \tag{73}$$

The special case $\alpha = 0$ or $\nu = \frac{1}{2}$ corresponds to a white spectrum and recovers the anomalous diffusion found previously by de Marsily and Matheron.[52]

Equation (68) with the kernel in Eq. (71) is a simple model of superdiffusive transport. Actually, there is a slightly more general model equation that contains these previous results as special cases and also subsumes various examples of subdiffusive transport. This model is

$$\partial_t g = \partial_x^2 \mathscr{I}^\nu f, \quad g = \mathscr{I}^\mu f, \quad g(x,0) = \delta(x), \tag{74}$$

where $0 \leqslant \mu, \nu \leqslant 1$, and the integral of fractional order is an operator defined by

$$\mathscr{I}^\xi f \equiv \int_0^t \frac{f(x,\tau)\,d\tau}{\Gamma(\xi)(t-\tau)^{1-\xi}}. \tag{75}$$

The first three nonzero spatial moments of the system in Eq. (74) are

$$\int g\,dx = 1, \quad \int x^2 g\,dx = \frac{2t^{2\beta}}{\Gamma(1+2\beta)}, \quad \int x^4 g\,dx = \frac{24t^{4\beta}}{\Gamma(1+4\beta)}, \tag{76}$$

where

$$\beta \equiv (1+\nu-\mu)/2. \tag{77}$$

Thus, apart from the subdominant term $2Dt$ in Eq. (73), our previous superdiffusive results are recovered when $\mu = 0$. Subdiffusive dispersion is obtained if $\nu = 0$ and, in this case, Eq. (74) reduces to transport equation studied by Young *et al.*[54] and Young.[45] In particular, the case $\nu = 0$ and $\mu = \frac{1}{3}$ describes the initial dispersion of passive scalar in an array of steady convection cells.

The kurtosis of the concentration is

$$\text{Ku} \equiv \frac{\int x^4 g\,dx}{(\int x^2 g\,dx)^2} = \frac{6\Gamma(1+2\beta)^2}{\Gamma(1+4\beta)}. \tag{78}$$

The Gaussian value $\text{Ku} = 3$ is recovered when $\beta = \frac{1}{2}$. If $\beta = 1$, we find that $\text{Ku} = 1$, which is consistent with the observation that Eq. (74) reduces to the wave equation when $\mu = 0$ and $\nu = 1$. Finally, when $\beta = 0$, we have $\text{Ku} = 6$. This is consistent with the symmetric exponential density, which is the solution of Eq. (74) in the limit $\nu = 0$ and $\mu \to 1$.

The expression in Eq. (78) for Ku is an exact consequence of Eq. (74). But the derivation of Eq. (74) is usually based on a wave-number expansion. Just as in Sec. II, there are additional terms, nonlocal in time and proportional to ∂_x^4, that appear on the right-hand side of Eq. (68) or (74) if the expansion is continued to higher order. The fourth spa-

tial moment cannot be correctly calculated without inclusion of these higher-order terms and explicit calculation of these requires consideration of the cubic and quartic statistical properties of the velocity field. Thus Eq. (78) with $\beta = \frac{3}{4}$ does not give the correct kurtosis for the problem posed by de Marsily and Matheron.[52] This quantity has been been calculated numerically by Bouchaud *et al*[55] and they found $\mathrm{Ku} \approx 3.3 \pm 0.03$.

The nonlocal transport equation in Eq. (68) is a good illustration of an important point: Complete transverse mixing does not ensure the validity of the Taylor diffusion equation. The initial condition $c'(x,z,0) = \delta(x)$ ensures that the tracer is uniformly mixed in the transverse direction, yet there is a prolonged regime of anomalous diffusion that lasts until times of order $(k_2^2 D)^{-1}$. On this very long time scale, the algebraic decay of the kernel in Eq. (71) changes to an exponential decay, and one recovers Taylor's result in Eq. (69). This slow adjustment is required so the most slowly decaying modes in Eq. (65) come into quasistatic equilibrium and this condition is not the same as thorough transverse mixing. From a Lagrangian point of view, this is also the time required for every fluid element to diffuse across the random velocity field and sample the complete range of transverse variations in speed.

The Lagrangian sampling condition leads to a simple heuristic argument, which explains the connection between the spectral slope α in Eq. (70), and the anomalous diffusion exponent $1 + \nu = (\alpha + 3)/2$ in Eq. (73). In a time t, a particle will have diffused through a transverse distance that scales as $(Dt)^{1/2}$ and will have sampled velocity variations with wavelengths less than this length scale. Thus, in the integral that defines Taylor's effective diffusivity, Eq. (69), there is a low wave-number cutoff that decreases as $(Dt)^{-1/2}$. With the spectral shape in Eq. (70), this gives $D_{\mathrm{eff}} \sim t^{(\alpha+1)/2}$. Finally, $\dot{\sigma}^2 \sim D_{\mathrm{eff}}$ leads to the anomalous diffusion law in Eq (73).

C. Logarithmic effects due to the no-slip condition

We turn now to an alternative model of anomalous diffusion in a unidirectional velocity field. This model identifies a subtle mechanism for preasymptotic dispersion, which relies on the no-slip condition at solid surfaces. This process results in "mildly anomalous" diffusion in which the variance of tracer with no molecular diffusivity grows as $t \ln t$. This serves as a warning that anomalous diffusion is not always characterized by power laws such as Eq. (49), and, in experimental or field data, the logarithm is insidious.

The logarithmic anomalous diffusion produced by the no-slip condition is illustrated with a kinematic construction that we call the "scrambler model." It is a pedagogical simplification of Saffman's[56] model of a consolidated porous medium. Saffman considered a random network of capillaries through which viscous fluid is pumped by a large-scale pressure gradient. The capillaries meet at nodes and it is assumed that perfect mixing takes place at these junctions where different tubes meet. (Shear dispersion in an individual capillary is unimportant if the average transit time through a capillary l/U is much less than the cross-sectional diffusion time a^2/D. Throughout this subsection we ensure this condition by taking $D = 0$.) With this model, Saffman identified two mechanisms that are responsible for a protracted nondiffusive regime. First, some capillaries are oriented almost at right angles to the pressure gradient and, consequently, are almost stagnant. Second, the no-slip condition at the capillary walls ensures that some tracer is retained in a particular capillary for a very long time.

We introduce the one-dimensional simplification of Saffman's model shown in Fig. 5. Tracer particles are advected down a channel by a Couette flow. The longitudinal coordinate is x and the transverse coordinate is y. The velocity is

$$u(y) = 2y \quad \text{where} \quad 0 \leqslant y \leqslant 1. \tag{79}$$

The tracer particles remain on the same streamline until they hit a "scrambler." The scramblers are located at $x = 1,2,3,\ldots$, and are thought of as perfect black box mixers whose input is a concentration of particles that depends on y and whose output is uniform concentration. Inside the black box, we imagine some device that rapidly and efficiently homogenizes the tracer passing through the scrambler so that the exit concentration is independent of y. Thus the scramblers are analogous to the capillary junctions in Saffman's more complicated model. The scrambler model isolates the effect of the no-slip boundary condition by eliminating the geometric complications of stagnant side branches.

The scrambler model is simulated numerically by starting an ensemble of particles at $x = 0$. Each particle has a different random y coordinate, picked uniformly between 0 and 1. Thus a particle whose initial ordinate is y_0 hits the first scrambler at $x = 1$ when $t = 1/2y_0$. It then instantly emerges at a new random value of y, say y_1. The correct specification of the probability density function (pdf) of the random variable y_1 is important. One must realize that, although the *concentration* of particles leaving the scrambler is independent of y, the *flux* is not. Because the flux is the number of particles per time emerging at a particular value of y, it is the flux that determines the relative likelihood of different exit locations.

Now, the flux of particles leaving the first scrambler is the product of the uniform exit concentration and the veloc-

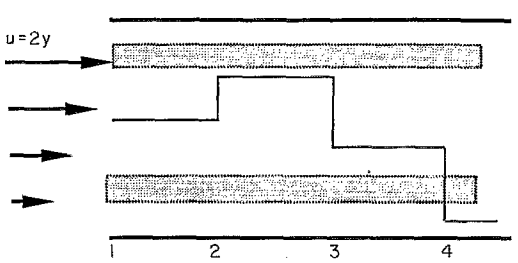

FIG. 5. An illustration of the scrambler model. Particles move downstream in the Couette flow $u = 2y$ and change streamlines at the scramblers located at $x = 1,2,\ldots$. The prescription for the pdf of exit ordinates in Eq. (60) ensures that particles spend equal times in equal areas, such as the two shaded regions above. However, the occupancy statistics are different. Particles pass through the upper region frequently but do not stay long. Particles enter the lower domain infrequently but stay for a long time before reaching the next scrambler.

ity at this exit is $u = 2y$. Thus particles leave more frequently where the velocity is larger. In fact, the pdf of exit ordinates, denoted by $\mathscr{Q}(y)$, is just proportional to $u(y)$. Thus, assuming for the moment a general velocity profile that is monotonic with y and positive [i.e., $u(y) \geqslant 0$], the pdf of exit ordinates after a scrambler is

$$\mathscr{Q}(y) = u(y)\left(\int_0^1 u(y)dy\right)^{-1}. \tag{80}$$

With $u(y) = 2y$, the normalization constant in the denominator of Eq. (63) is equal to one and the pdf of exit ordinates is just $2y$.

The particle eventually hits the next scrambler at $x = 2$ and the ordinate y is reset again by random selection from the density in Eq. (80). Thus each particle in the ensemble moves down the channel changing its y coordinate only when it strikes a scrambler. After striking a scrambler, it is more likely to emerge where the velocity is larger. Of course, if a particle does happen to emerge near the lower boundary, then it takes a very long time to reach the next scrambler. In the meantime, the center of mass of the ensemble moves downstream with the sectionally averaged velocity $U = 1$. Thus particles near the no-slip boundary move with a speed $u' \equiv u(y) - U \approx -1$ relative to the center of mass, and do so for long periods of time.

Figure 6 shows histograms of particle positions obtained from a numerical simulation of the scrambler model with $N = 20\,000$ particles at $t = 10\,000$. The particles are distributed uniformly in the transverse direction and usually this would be taken as *prima facie* evidence that the diffusive Taylor limit has been reached. In the longitudinal direction x, the peak concentration is at $x = Ut = 10\,000$ as expected. However, the distribution is skew and non-Gaussian. In Fig. 8, we show the variance divided by $2t$. If the dispersion were diffusive, as in the Taylor limit, this would approach a constant. Actually, it increases as $\ln t$.

To explain this logarithmic dispersion, we begin with Taylor's[7] expression for the rate of change of the variance in terms of the Lagrangian velocity autocorrelation function

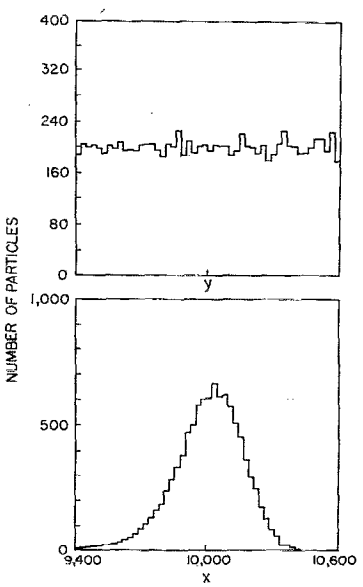

FIG. 6. This shows histograms of particle positions produced by a simulation of the scrambler model at $t = 10\,000$. There are $N = 20\,000$ particles in the ensemble. The upper panel shows that transverse mixing is complete. The lower panel shows the skew distribution that develops as the ensemble moves downstream. The mean position is $x = Ut = 10\,000$.

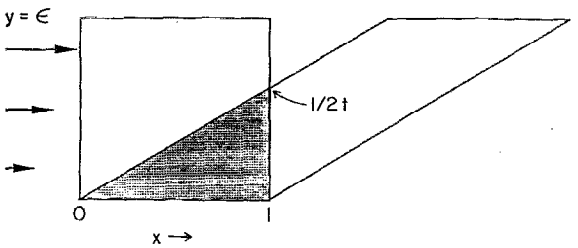

FIG. 7. Initially, the area in a strip $0 < x < 1$ and $0 < y < \epsilon$ (the square) is uniformly occupied by particles. Because of differential advection at t, only the stippled area contains particles that were in the strip initially. Thus the fraction of particles that remain in the strip for the entire interval $(0,t)$ is the ratio of the area of the stippled triangle to the square, i.e., $1/4t\epsilon$.

$$\frac{d\sigma^2}{dt} = 2\int_0^t \mathscr{C}(t_1)dt_1. \tag{81}$$

Here,

$$\mathscr{C}(t) \equiv \frac{1}{N}\sum_{i=1}^{i=N} u_i'(0)u_i'(t) \tag{82}$$

is the ensemble average of the velocities relative to the center of mass. Because of the logarithmic growth of variance in the scrambler model, we must have

$$\mathscr{C}(t) \sim p/t \tag{83}$$

as $t \to \infty$.

We can calculate p by considering a thin strip $0 < y < \epsilon \ll 1$ near the boundary. At any time, say $t = 0$, a fraction ϵ of the N particles in the ensemble are in this strip. All of these particles have a velocity $u' \approx -1$ relative to the center of mass. At some distant time t in the future, most of the particles in the ensemble will have passed through a scrambler and "forgotten" their velocities at $t = 0$. However, a certain fraction of the slow moving particles in the strip will not yet have encountered the next scrambler. This fraction is easy to calculate geometrically as in Fig. 7 and is equal to the ratio of the area of unevacuated region, $1/4t$, to the initial area of the strip ϵ.

Long time correlations are due to these particles that haven't passed through a scrambler and, as $t \to \infty$, the only nonzero terms in the sum in Eq. (82) come from particles that remained in the strip for the whole interval. For these particles, $u'(0)u'(t) = (-1)^2$ and so the correlation function is

$$\mathscr{C}(t) \approx \left(\frac{1}{N}\right)(\epsilon N)\left(\frac{1}{4t\epsilon}\right)(-1)^2 = \frac{1}{4t}. \tag{84}$$

The first factor on the right-hand side of Eq. (84) is the division by the total number of particles in the ensemble. The second factor is the number of particles in the strip at $t = 0$. The third factor is the fraction of these particles that still remain in the strip at t. The product of the second and third factors is the number of nonzero terms in the sum in (82). The final factor $(-1)^2$ is the value of each of these terms.

Thus the correlation function decays slowly as in Eq. (83) with $p = \frac{1}{4}$. From Eq. (81), it follows that σ^2 grows as $\frac{1}{2}t \ln t$. This result is compared with the simulation in Fig. 8 and with an exact solution in the Appendix. We emphasize

that the $t \ln t$ growth of variance is a consequence of the no-slip condition at $y = 0$. Repeating the simulation with velocity fields that slip at both boundaries results in a normal diffusion process with $\sigma^2 \sim t$. Also, returning to the no-slip case, if the tracer has a very small molecular diffusivity, then the $t \ln t$ regime is transient and is replaced by true diffusion at very large times. This happens because molecular diffusion accelerates the evacuation of the strip in Fig. 8 and results in an exponential decrease in $\mathscr{C}(t)$ as $t \to \infty$.

The scrambler model shows, once again, that complete transverse mixing is not sufficient for the validity of the Taylor limit and also that anomalous diffusion does not always result in power laws such as Eq. (49). The principal point is that, without molecular diffusion, the Taylor limit is never reached because there are always a significant number of particles that are trapped near the walls and so have not sampled the entire cross section of the flow.

The relevance of this scrambler model to dispersion in rivers is not at all obvious, but there are some similarities between the skew distribution in Fig. 6 and observations such as those in Fig. 2. However, the $t \ln t$ growth of variance is not consistent with field observations that show a definite power law, such as Eq. (49), often with β as large as 1.[41,43]

V. CONCLUSIONS

In this review, we have emphasized the asymptotic nature of the Taylor diffusion approximation. It is valid only at large times when the rapidly decaying modes, with nontrivial transverse structure, have reached a quasistatic equilibrium and so can be treated as slave variables. An asymptotic formulation, based the center manifold theorem,[12] leads to a wave-number expansion in which the errors in the spatial moments and cumulants are exponentially small as $t \to \infty$.

However, this description fails to explain observations of superdiffusive dispersion in rivers. We conclude that, in tracer release experiments in rivers, the exponential transients continue to be important over the observational time scales. Indeed, Smith[21,48] has given a multimode formulation of tracer transport in unidirectional shear flows and he has also presented a time delay formulation[16] that implicitly contains information about these exponentially decaying modes. However, these models have not yet led to an explanation for a prolonged regime of superdiffusive spreading in rivers. For this reason, we have found it interesting to examine a multimode formulation of the de Marsily and Matheron[52] model of superdiffusive dispersion in aquifiers. In this context, it is a quasicontinuous superposition of slowly decaying exponential transients whose sum is an *algebraically* decaying kernel, such as Eq. (71), that results in the superdiffusive dispersion. It is the algebraic decay of the kernel that distinguishes this model from the exponentially decaying kernel in Ref. 16. It is also clear that a quasicontinuous sum of exponentially decaying modes is required to construct an algebraically decaying kernel, which is why the finite truncations in Refs. 21 and 48 do not produce superdiffusive dispersion. Thus an outstanding unsolved problem is the construction of a theoretical model that accounts for field observations of superdiffusive dispersion in rivers by identifying the physical mechanism that produces a continuum of slowly decaying modes.

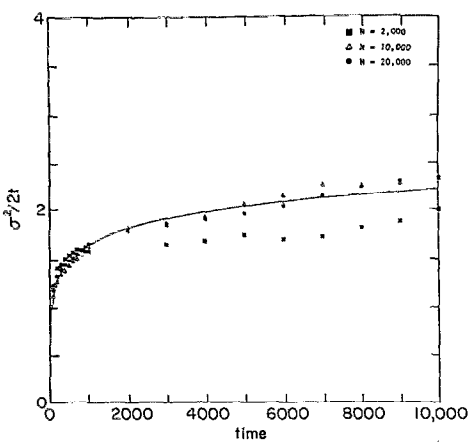

FIG. 8. This figure shows a comparison of three simulations using different numbers of particles. The solid curve is the theoretical result from Eq. (A25) with $\beta = 1$.

ACKNOWLEDGMENTS

We thank the San Diego Supercomputer Center for a computing resources and Joel Koplik and Steve Cox for some interesting conversations on this material.

Scott Jones is supported by the Air Force Office of Scientific Research under Contract No. AFOSR-89-0226. W. R. Young is supported by National Science Foundation Contract No. NSF-OCE-9006430 and Office of Naval Research Contract No. ONR-N00014-90-J-1201.

APPENDIX: EXACT SOLUTION OF THE SCRAMBLER MODEL

Our simulation of the scrambler model uses the Lagrangian approach described in the text. In this appendix, we use an Eulerian formulation and obtain some exact results for this model. The most important result in this appendix is an exact expression for the variance in Eq. (A25). This result confirms the heuristic argument leading to Eq. (84).

In Eulerian terms, the fundamental variable is the concentration of tracer $c(x,y,t)$. In between the scramblers, this function evolves according to the advection equation with no molecular diffusivity

$$\partial_t c + 2y\partial_x c = 0. \tag{A1}$$

The scramblers provide boundary conditions for this equation at $x = 1,2,3,\ldots$. Just to the *right* of the nth scrambler, at $x = n$,

$$c_R(n,y,t) = \alpha_n(t), \tag{A2}$$

where $\alpha_n(t)$ is the uniform concentration obtained by mixing the tracer entering the scrambler from the left. Conservation of tracer gives

$$\alpha_n(t) = \int_0^1 2y c_L(n,y,t)\,dy, \tag{A3}$$

where, in the integral above, $c_L(n,y,t)$ is the concentration

just to the *left* of the nth scrambler. Equations (A1)–(A3) specify the scrambler model in Eulerian variables.

We begin by introducing the *inventory* of the segment between $x = n$ and $x = n + 1$. This is

$$\phi_n(t) \equiv \int c(x,y,t)\,dA_n, \tag{A4}$$

where the integral is over the domain $n < x < n + 1$ and $0 < y < 1$. Integrating (A1) over this same region gives

$$\begin{aligned} \partial_t \phi_0 &= -\alpha_1, \\ \partial_t \phi_1 &= \alpha_1 - \alpha_2, \\ \partial_t \phi_2 &= \alpha_2 - \alpha_3, \end{aligned} \tag{A5}$$

and so on. The physical interpretation of this system is straightforward, viz., the tracer that leaves one segment appears in its neighbor downstream.

Next, we solve Eq. (A1) with the boundary condition in Eq. (A2). The solution is

$$c(x,y,t) = \alpha_n[t - (x - n)/2y], \quad \text{if } n < x < n + 1. \tag{A6}$$

This result, evaluated at $x = n + 1$, is now used in Eq. (A3) to relate $\alpha_{n+1}(t)$ to $\alpha_n(t)$. One finds

$$\alpha_{n+1}(t) = \int_0^1 2y\alpha_n\left(t - \frac{1}{2y}\right) dy, \tag{A7}$$

or by changing the variables to $\tau = 1/2y$ and using $\alpha_n(t) = 0$ if $t < 0$, we can rewrite this as a convolution

$$\alpha_{n+1}(t) = \int_0^t \mathscr{P}(\tau)\alpha_n(t - \tau)\,d\tau, \tag{A8}$$

where

$$\begin{aligned} \mathscr{P}(\tau) &\equiv 1/2\tau^3, \quad \text{if } \tau \geqslant \tfrac{1}{2}, \\ \mathscr{P}(\tau) &\equiv 0, \quad \text{if } \tau < \tfrac{1}{2}. \end{aligned} \tag{A9}$$

The kernel $\mathscr{P}(\tau)$ can be interpreted as the probability density function of the residence time in a section of channel between two scramblers. This interpretation makes Eq. (A8) intuitively plausible. The number of particles that enter section n at $t - \tau$ is $\alpha_n(t - \tau)$ and a fraction $\mathscr{P}(\tau)d\tau$ of these eventually leave at a time τ later. Thus, in Eq. (A8), to calculate the total number leaving at t, one sums over the different arrival times in the past.

Because of the convolution in Eq. (A8), the Laplace transform

$$\tilde{\phi}_n(s) \equiv \int_0^\infty \phi_n(t)\exp(-st)\,dt \tag{A10}$$

immediately simplifies the system. If all of the tracer is initially in the first section, then the initial condition is

$$\phi_0(0) = 1 \quad \text{and} \quad \phi_n(0) = 0 \text{ if } n \neq 0 \tag{A11}$$

and the transform of Eq. (A5) is

$$\begin{aligned} s\tilde{\phi}_0(s) &= 1 - \tilde{\alpha}_1(s), \\ s\tilde{\phi}_1(s) &= \tilde{\alpha}_1(s) - \tilde{\alpha}_2(s), \\ s\tilde{\phi}_2(s) &= \tilde{\alpha}_2(s) - \tilde{\alpha}_3(s), \end{aligned} \tag{A12}$$

and so on. The transform of Eq. (A8) leads to

$$\tilde{\alpha}_n(s) = \tilde{\mathscr{P}}(s)^{n-1}\tilde{\alpha}_1(s). \tag{A13}$$

Putting Eq. (A13) into Eq. (A12), we have

$$\begin{aligned} s\tilde{\phi}_0(s) &= 1 - \tilde{\alpha}_1, \\ s\tilde{\phi}_1(s) &= \tilde{\alpha}_1(1 - \tilde{\mathscr{P}}), \\ s\tilde{\phi}_2(s) &= \tilde{\alpha}_1\tilde{\mathscr{P}}(1 - \tilde{\mathscr{P}}), \end{aligned} \tag{A14}$$

and so on.

It is now convenient to summarize this solution by forming spatial moments. The first of these is

$$\sum_{i=0}^{\infty} \tilde{\phi}_i = \frac{1}{s} \tag{A15}$$

and the inverse transform of this is just conservation of tracer. The next three spatial moments are

$$s\sum_{i=0}^{\infty} i\tilde{\phi}_i = \frac{\tilde{\alpha}_1}{1 - \tilde{\mathscr{P}}}, \tag{A16a}$$

$$s\sum_{i=0}^{\infty} i^2\tilde{\phi}_i = \frac{\tilde{\alpha}_1(1 + \tilde{\mathscr{P}})}{(1 - \tilde{\mathscr{P}})^2}, \tag{A16b}$$

$$s\sum_{i=0}^{\infty} i^3\tilde{\phi}_i = \frac{\tilde{\alpha}_1(1 + 4\tilde{\mathscr{P}} + \tilde{\mathscr{P}}^2)}{(1 - \tilde{\mathscr{P}})^3}. \tag{A16c}$$

To invert these transforms we use Tauberian theorems that relate the inverse transform at large values of t to the behavior of the transform at small values of s.

Expanding the right-hand sides when s is small, we begin by noting that, with $\mathscr{P}(t)$ in Eq. (A9),

$$\tilde{\mathscr{P}}(s) = 2E_3(s/2) \tag{A17a}$$

$$\approx 1 - s - \left(\frac{s}{2}\right)^2 \ln\left(\frac{s}{s_0}\right) + \frac{s^3}{24} + \cdots, \tag{A17b}$$

where E_3 is an exponential integral[57] and

$$s_0 \equiv 2e^{3/2 - \gamma} \approx 5.03 \quad \text{with } \gamma = 0.577\,21\cdots. \tag{A18}$$

The function $\alpha_1(t)$ depends on the details of how the tracer is distributed initially. In our simulation, $c(0,x,y) = \delta(x)$ and, calculating the flux of tracer out of the first segment at $x = 1$, one finds

$$\begin{aligned} \alpha_1(t) &= 0, \quad \text{if } t < \tfrac{1}{2}, \\ \alpha_1(t) &= 1/2t^2 \quad \text{if } t > \tfrac{1}{2}. \end{aligned} \tag{A19}$$

The Laplace transform of this is

$$\tilde{\alpha}_1(s) = E_2(s/2)$$

$$\approx 1 + (s/2)\,[\ln(s/2) - 1 + \gamma] + \cdots \tag{A20}$$

as $s \to 0$. One expects that, as $t \to \infty$, the initial distribution of the tracer does not affect the behavior of the center of mass or the mean square displacement σ^2. However, this is not clear until the end of the asymptotic analysis and, in order to treat a wide class of initial conditions, we assume that as $s \to 0$ the function $\tilde{\alpha}_1(s)$ behaves like

$$\tilde{\alpha}_1(s) \approx 1 + s^\beta\mu_1(s) + s^{\beta+1}\mu_2(s) + \cdots, \tag{A21}$$

where μ_1 and μ_2 are "slowly varying" functions such as constants or logarithms. The expansion in (A20) is an example of this with $\beta = 1$. To order the following asymptotic expansions, it is convenient to assume that $\beta \geqslant 1$. As an ex-

ample of initial conditions that violate this inequality, we note that, if $c(x,y,0) \propto y^{-\lambda}$ as $y \to 0$, then $\beta = 1 - \lambda$. Thus, if the initial condition has an infinite, but integrable, concentration near the no-slip boundary, then β may be less than 1. This unphysical case is excluded from the discussion below.

Substituting Eqs. (A17b) and (A21) into Eq. (A16b) gives

$$\sum_{i=0}^{\infty} i\tilde{\phi}_i(s) = \frac{1}{s^2} - \left(\frac{1}{4s}\right)\ln\left(\frac{s}{s_0}\right) + s^{\beta-2}\mu_1(s) + \cdots \tag{A22}$$

so that, as $t \to \infty$,

$$\sum_{i=0}^{\infty} i\phi_i(t) \approx t + \frac{1}{4}\ln(s_0 t) + \left(\frac{t^{1-\beta}\mu_1(1/t)}{\Gamma(2-\beta)}\right) + \cdots . \tag{A23}$$

The first term on the right-hand side of the above is the motion of the center of mass with the sectionally averaged velocity in the channel. Provided that $\beta \geqslant 1$, the remaining two terms are subdominant as $t \to \infty$ however, they must be retained for a consistent calculation of σ^2.

Next, expanding the right-hand side of Eq. (A16b), and inverting the transform, we find that

$$\sum_{i=0}^{\infty} i^2\phi_i(t) \approx t^2 + t\ln(s_0 t) - t + \left(\frac{2t^{2-\beta}\mu_1(1/t)}{\Gamma(3-\beta)}\right) + \cdots . \tag{A24}$$

Combining Eqs. (A22) and (A23), we now have, as $t \to \infty$,

$$\sigma^2(t) \approx \sum_{i=0}^{\infty} i^2\phi_i(t) - \left(\sum_{i=0}^{\infty} i\phi_i(t)\right)^2,$$

$$\approx \frac{1}{2}t\ln(s_0 t) - t + \frac{2(\beta-1)t^{2-\beta}\mu_1(1/t)}{\Gamma(2-\beta)} + \cdots . \tag{A25}$$

The last term in the equation above isolates the possible asymptotic influence of the initial conditions. Provided that $\beta \geqslant 1$, this term is subdominant and, in the important case $\beta = 1$, it vanishes. Thus the initial conditions do not effect the asymptotic properties of the dispersion process. The remaining terms on the right-hand side show that the growth of variance is anomalous and it is this analytic result that is compared with numerical simulation in Fig. 8. The leading term $\frac{1}{2}t\ln t$ corresponds to a velocity autocorrelation function with the asymptotic structure in Eq. (84).

[1] G. I. Taylor, Proc. R. Soc. London Ser. A **219**, 186 (1953).
[2] R. Aris, Proc. R. Soc. London Ser. A **235**, 67 (1956).
[3] R. Smith, J. Fluid Mech. **114**, 379 (1982).
[4] W. R. Young, P. B. Rhines, and C. J. R. Garrett, J. Phys. Oceanogr. **12**, 515 (1982).
[5] G. K. Batchelor, J. Fluid Mech. **106**, 1 (1981).
[6] G. I. Taylor, Proc. R. Soc. London Ser. A **223**, 446 (1954).
[7] G. I. Taylor, Proc. London Math. Soc. **20**, 196 (1921).
[8] P. C. Chatwin, J. Fluid Mech. **48**, 689 (1971).
[9] P. C. Chatwin and C. M. Allen, Annu. Rev. Fluid Mech. **17**, 119 (1985).
[10] A. J. Roberts, J. Aust. Math. Soc. B **29**, 480 (1988).
[11] A. J. Roberts, J. Aust. Math. Soc. B **31**, 48 (1989).
[12] G. N. Mercer and A. J. Roberts, SIAM J. Appl. Math. **50**, 1547 (1990).
[13] S. M. Cox and A. J. Roberts, to appear in J. Aust. Math. Soc. B.
[14] I. Frankel and H. Brenner, J. Fluid Mech. **204**, 97 (1989).
[15] P. C. Chatwin, J. Fluid Mech. **43**, 321 (1970).
[16] R. Smith, J. Fluid Mech. **105**, 469 (1981).
[17] M. E. Erdogan and P. C. Chatwin, J. Fluid Mech. **29**, 465 (1967).
[18] E. A. Spiegel and S. Zaleski, Phys. Lett. A **106**, 335 (1984).
[19] J. Carr, *Applications of Center Manifold Theory* (Springer-Verlag, New York, 1981).
[20] W. N. Gill and R. Sankarasubramanian, Proc. R. Soc. London Ser. A **316**, 341 (1970).
[21] R. Smith, J. Fluid Mech. **175**, 201 (1987).
[22] D. L. Koch and J. F. Brady, Chem. Eng. Sci. **42**, 1377 (1987).
[23] R. Smith, IMA J. Appl. Math. **28**, 149 (1982).
[24] D. E. Cormack, L. G. Leal, and J. Imberger, J. Fluid Mech. **65**, 209 (1974).
[25] D. E. Cormack, L. G. Leal, and J. H. Seinfeld, J. Fluid Mech. **65**, 231 (1974).
[26] J. Imberger, J. Fluid Mech. **65**, 247 (1974).
[27] C. J. Chapman and M. R. E. Proctor, J. Fluid Mech. **101**, 759 (1980).
[28] A. J. Roberts, J. Fluid Mech. **158**, 71 (1985).
[29] C. Depassier and E. A. Spiegel, Geophys. Astrophys. Fluid Dyn. **21**, 167 (1982).
[30] R. Smith, J. Fluid Mech. **78**, 677 (1976).
[31] J. S. Godfrey, Estuarine Coastal Mar. Sci. **11**, 295 (1980).
[32] D. W. Pritchard, J. Mar. Res. **11**, 106 (1952).
[33] D. W. Pritchard, J. Mar. Res. **13**, 133 (1954).
[34] D. W. Pritchard, J. Mar. Res. **14**, 33 (1956).
[35] E. Guyon, J.-P. Nadal, and Y. Pomeau, *Disorder and Mixing* (Kluwer Academic, Dordrecht, 1987).
[36] D. L. Koch and J. F. Brady, J. Fluid Mech. **154**, 399 (1985).
[37] D. L. Koch and J. F. Brady, Phys. Fluids **31**, 965 (1988).
[38] D. L. Koch and J. F. Brady, Phys. Fluids A **1**, 47 (1989).
[39] C. F. Nordin and G. V. Sabol, Water Resour. Inves. **20–74**, 332 pp. (1974).
[40] C. F. Nordin and B. M. Troutman, Water Resour. Res. **16**, 123 (1980).
[41] T. J. Day, Water Resour. Res. **11**, 909 (1975).
[42] E. M. Valentine and I. R. Wood, J. Hydraul. Div., Am. Soc. Civil Eng. **103**, 975 (1977).
[43] T. J. Day and I. R. Wood, Water Resour. Res. **12**, 655 (1976).
[44] S. Sundersan, N. R. Amundson, and R. Aris, Am. Inst. Chem. Eng. J. **26**, 529 (1980).
[45] W. R. Young, J. Fluid Mech. **193**, 129 (1988).
[46] A. Purnama, J. Fluid Mech. **186**, 351 (1988).
[47] A. Purnama, J. Fluid Mech. **195**, 393 (1988).
[48] R. Smith, J. Fluid Mech. **178**, 257 (1987).
[49] E. W. Montroll and M. F. Shlesinger, in *Nonequilibrium Phenomena II*, edited by J. L. Lebowitz and E. W. Montroll (Elsevier, Amsterdam 1984).
[50] E. W. Montroll and B. J. West, in *Fluctuation Phenomena*, edited by E. W. Montroll and J. L. Lebowitz (North-Holland, Amsterdam, 1979).
[51] J. W. Haus and K. W. Kehr, Phys. Rep. **150**, 263 (1987).
[52] G. de Marsily and G. Matheron, Water Resour. Res. **16**, 901 (1980).
[53] R. E. Davis, J. Mar. Res. **45**, 635 (1987).
[54] W. R. Young, A. Pumir, and Y. Pomeau, Phys. Fluids A **1**, 462 (1989).
[55] J.-P. Bouchaud, A. Georges, J. Koplik, A. Provata, and S. Redner, Phys. Rev. Lett. **64**, 2503 (1990).
[56] P. G. Saffman, J. Fluid Mech. **6**, 321 (1959).
[57] *Handbook of Mathematical Functions*, edited by M. Abramowitz and I. Stegun (Wiley–Interscience, New York, 1972).